Research Square

Preprints are preliminary reports that have not undergone peer review.
They should not be considered conclusive, used to inform clinical practice,
or referenced by the media as validated information.

Developmental trajectories of neural modules underlying emotion generation and regulation across childhood and adolescence

Xi Chen

xchen@psy.ecnu.edu.cn

School of Psychology and Cognitive Science, East China Normal University

Cong Xia

School of Psychology and Cognitive Science, East China Normal University

Ximu He

School of Psychology and Cognitive Science, East China Normal University

Qing Ma

East China Normal University

Xutong Zhang

School of Psychology and Cognitive Science, East China Normal University

Cong Xie

East China Normal University

Ning Hao

East China Normal University

Yi Luo

East China Normal University https://orcid.org/0000-0002-6169-8938

Rui Ding

IDG/McGovern Institute for Brain Research & State Key Laboratory of Cognitive Neuroscience and Learning

Shaozheng Qin

State Key Laboratory of Cognitive Neuroscience and Learning & International Data Group/McGovern Institute for Brain Research, Beijing Normal University, Beijing https://orcid.org/0000-0002-1859-2150

Article

Keywords: Emotion regulation; Emotion generation; Neural modules; fMRI

Posted Date: November 2nd, 2026

DOI: https://doi.org/10.21203/rs.3.rs-11180725/v1

License: This work is licensed under a Creative Commons Attribution 4.0 International License.
Read Full License

Additional Declarations: There is **NO** Competing Interest.

Developmental trajectories of neural modules underlying emotion generation and regulation across childhood and adolescence

Cong Xia[1†], Ximu He [1†], Xi Chen [1*], Qing Ma [1], Xutong Zhang[1], Cong Xie[1], Ning Hao[1], Yi Luo[1], Rui Ding[2], Shaozheng Qin[2]

[1]The school of psychology and cognitive science, East China Normal University, Shanghai, China

[2]State Key Laboratory of Cognitive Neuroscience and Learning & IDG/McGovern Institute for Brain Research, Beijing Normal University, Beijing, China

[†]These authors contributed equally to the work and should be considered co-first authors.

***Corresponding Author:**

*Correspondence concerning this article should be addressed to Xi Chen, School of Psychology and Cognitive Science, East China Normal University, Shanghai, China, Email: xchen@psy.ecnu.edu.cn.

Abstract

Emotional maturation involves a fundamental shift from the raw, somatic reactions during childhood to the precise, cognitively elaborated processes during adulthood. However, the neural dynamics that drive this developmental transition, especially the changing contributions of distributed neural modules, remain unclear. Leveraging principal component analysis of a large-scale fMRI dataset in conjunction with a sliding-window regression approach, we quantified age-varying contributions of neural modules to emotion generation and emotion regulation. During emotion generation, while frontotemporal modules are the predominant sources of activation, the limbic-salience module remains the core substrate contributing to negative affect across the entire age range. For emotion regulation via reappraisal, the lateral temporal module emerged as the sole positive contributor to regulatory success. Conversely, activation of the frontotemporal regions around age 8 and the occipital activation across the entire age range contributed to poorer regulation. Such modules further showed distinct linear and quadratic links to real-world emotion measures and cross-process coupling. Together, the work delineates a dynamic, non-linear reorganization of emotional architecture and underscores the need for stage-matched interventions.

Keywords: Emotion regulation; Emotion generation; Neural modules; fMRI

Introduction

The maturation of human emotion is not a linear scaling of innate responses, but a fundamental transition in the brain's functional architecture. This trajectory marks a qualitative shift from the automatic, stimulus-driven reactions during early childhood to the highly integrated, semantic-driven processes during adulthood[1–3]. Such a reorganization requires the dynamic integration of multiple high-level processes including executive functions and social cognition, which reconfigure the neural processes underlying emotional functioning [4–9]. In early childhood, emotion generation is heavily anchored in subcortical and limbic circuitry[10]. In contrast, emotion regulation depends on the protracted development of the prefrontal cortex (PFC)[11,12]. During adolescence, the dual-systems model posits that the developmental mismatch between the rapidly maturing limbic system and laggard prefrontal control contributes to the heightened emotional sensitivity observed during adolescence[13–16]. Complementing this view, the social reorientation framework suggests that pubertal maturation triggers a neural reorganization toward enhanced sensitivity to social and affective cues, shifting processing from subcortical to higher-order cortical networks[17]. Such transition may continue into adulthood, as adults increasingly recruit higher-order regions such as the posterior superior temporal sulcus (pSTS) for social-semantic evaluation and context extraction[18]. Critically, the functional contribution of specific neural modules is hypothesized to undergo nonlinear reorganization across childhood and adolescence. However, direct empirical evidence for how such modular contributions evolve across the full developmental spectrum remains scarce.

Despite the explanatory power of the dual-systems and social reorientation frameworks, they have primarily been tested through region-of-interest approaches that conflate neural activation with functional contribution. A fundamental question remains which specific neural modules exert dominant contributions to emotion generation and regulation across developmental stages[17,19]. Progress in understanding these mechanisms has been hampered by a focus on regional activation that provides indirect evidence of functional importance. Crucially, BOLD activation levels do not inherently equate to functional contribution[20]. High activation magnitude may represent neural inefficiency, where immature regions exhibit hyper-activation as they struggle to meet task demands. To fully deconstruct the development of emotional functioning, we must move beyond activation

maps and directly quantify how the contribution weights of specific neural modules to emotion generation and regulation change across the developmental spectrum.

Characterizing these developmental processes is further challenged by the limitations of small-scale studies and discrete age-group comparisons. Existing research often lacks the statistical robustness and unified paradigms required to delineate the continuous developmental spectrum from childhood through late adolescence. Linear models fail to capture the complex, non-linear trajectories of functional reorganization. A large-scale, fine-grained approach is essential to resolve how neural modules dynamically alternate as drivers of emotional generation and regulation as suggested by the dual-systems and social reorientation frameworks.

In the current study, we addressed this challenge by leveraging a large-scale fMRI dataset (*N*=1,464, age range = 6–19 years, from China Child Brain Development Project) to identify the neural modules underlying emotion generation and regulation and to visualized their contributions across the age range. Participants in this study viewed negative faces without reappraisal ('Look negative'), neutral faces ('Look neutral') and a matched set of negative faces with reappraisal ('Regulate negative') during scanning (**Fig.1 Step1**). We first constructed contrast maps of emotion generation ('Look negative' – 'Look neutral') and emotion regulation ('Regulate negative' – 'Look negative'). To identify critical neural modules associated with emotion generation and regulation, we performed Principal Component Analysis (PCA) on voxels in each contrast mask. Spatial maps were generated by assigning each voxel to the PC (Principal component) with the highest positive loading, and individual PC scores were calculated (**Fig.1 Step2**). To quantify the fine-grained age-related contribution of these neural modules to individual differences in emotion generation and regulation, we employed a sliding window approach (window size = 2 years, step size = 0.25 years) across the full age range of the sample (Supplementary Fig. 1). Within each sliding window, we fitted multiple regression models to predict task performance (emotion generation effect: difference in self-reported negative affect between 'Look negative' and 'Look neutral'; emotion regulation effect: difference in self-reported negative affect between 'Look negative' and 'Regulate negative') from the z-scored activation of all corresponding PCs. The contribution of each PC was quantified as the product of the variance it explained (R^2) and the direction (sign) of its regression coefficient (Fig.1 Step3). To characterize the functional roles of these neural modules, we used two

complementary approaches. First, we functionally annotated these modules by correlating their spatial maps with Neurosynth topic maps (based on 11,406 studies), linking these modules to psychological processes. Second, we examined their linear and quadratic associations with various emotion-related measures.

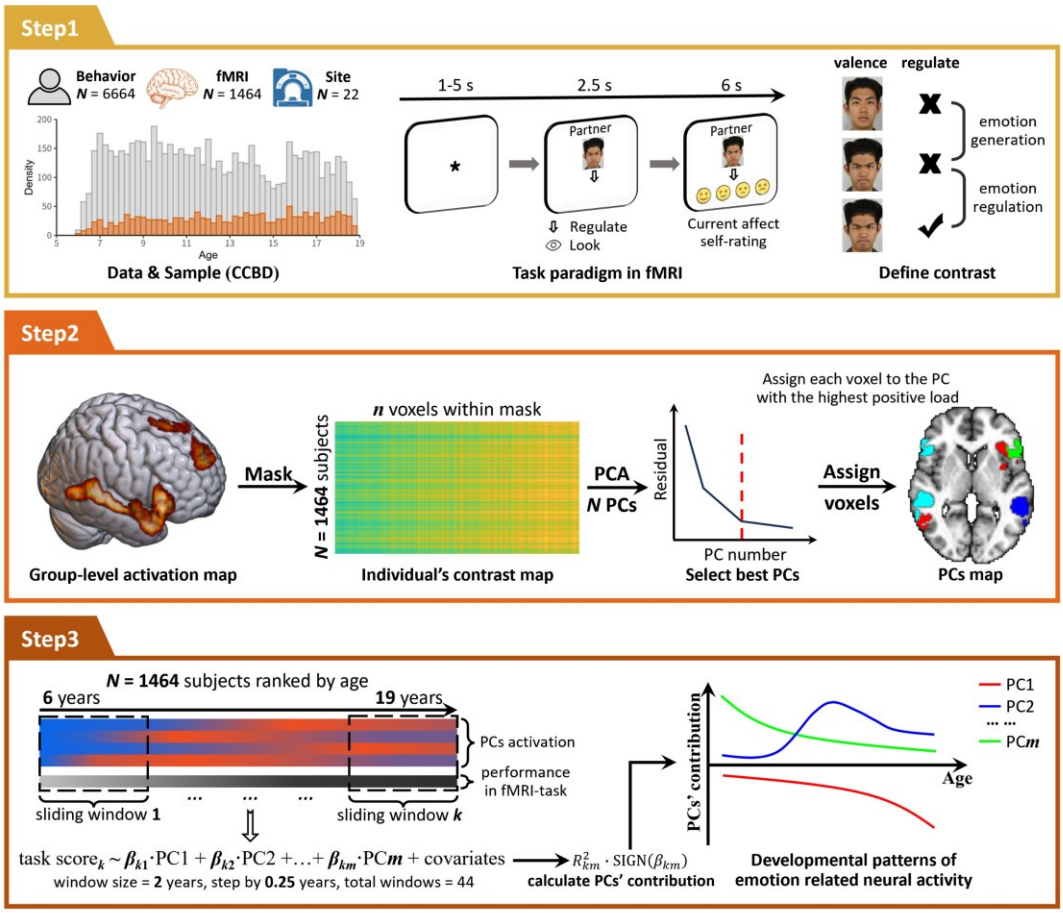


Fig. 1 Overview of the experimental paradigm and analysis pipeline. Step 1: Sample size and task paradigm. Participants completed trials, in which they viewed an image with an appraisal cue ('Look' or 'Decrease'), followed by a rating of self-experienced negative affect. **Step 2: fMRI analysis workflow.** Contrast maps for each task condition in each individual were extracted using a group-level activation mask. PCA was applied to the masked data, with the optimal number of modules determined using a scree plot, yielding spatial maps and individual PC scores. **Step 3: Algorithm of contribution.** Within each window, multiple regression models were fitted to quantify the contribution of PCs to task performance across development.

Results

Behavioral results

Reappraisal attenuates negative affect. Using a generalized linear mixed model (GLMM) to account for subject-level variability and scanner effects, we examined the impact of regulation on self-reported negative affect. Compared with the 'Look negative', participants reported lower negative affect during the 'Regulate negative' condition (β = -0.018, *SE* = 0.009, *t* = -2.05, *p* = 0.040). As a manipulation check, 'Look negative' also elicited significantly higher ratings of negative affect than 'Look neutral' (β = -0.053, *SE* = 0.010, *t* = -5.47, *p* < 0.001). Reaction times in 'Look negative' were longer than in 'Look neutral' (β = 0.024, *SE* = 0.006, *t* = -3.97, *p* < 0.001) and shorter than in 'Regulate negative' (β = -0.048, *SE* = 0.006, *t* = 8.03, *p* < 0.001).

Contribution of four PCs to emotion generation across development

We obtained activation and deactivation maps for emotion generation when passively viewing negative facial expressions (Supplementary Fig. 2-3). Based on the elbow criterion, the neural activation patterns were optimally decomposed into four distinct components via PCA (Supplementary Fig. 5). In parallel, PCA applied to the deactivation map yielded two distinct components, which primarily encompassed the occipital pole and lateral occipital cortex (Supplementary Table 6). Detailed results of these deactivation components are provided in the Supplementary Materials (Supplementary Fig. 6-8 and Supplementary Table 7, 11).

PC1 anchored onto the bilateral temporal poles, the middle temporal gyri, the inferior temporal gyri, amygdala and anterior insular cortex (Fig.2 Top-right and Supplementary Table 2) and was named as the limbic-salience module. PC1 showed a significant positive contribution to the emotion generation effect across all age windows (Fig.2 Top-left). The activation of PC1 was the lowest among the four PCs from age 8 onward (Fig.2 Bottom-left and Supplementary Table 1). Voxels of this module exhibited a bilaterally distributed profile characterized by substantial overlap with the ventral attention network (VAN) (LH: 23.8%; RH: 7.7%) and limbic network (LN) (~17% bilaterally), alongside notable subcortical engagement (~4.9%) (Fig.2 Bottom-left). In contrast, the other three PCs displayed strong hemispheric lateralization anchored in the default mode network

(DMN).

PC2 anchored onto the left dmPFC, left OFC and bilateral p-insular cortex (Fig.2 Top-right) and was named as the left frontal module. PC2 exhibited a distinct developmental profile, exerting a significant negative contribution to the emotion generation effect during two specific developmental windows: mid-childhood (8–10.5 years) and adolescence (12–16.5 years) (Fig.2 Top-left). Furthermore, the activation of PC2 was higher than that of PC1 from 8 years of age and peaked at 12 and 17 years (Fig.2 Bottom-left). Anatomically, this module was predominantly localized to. Voxels were predominantly localized to the left DMN (69.3%) and left Control Network (10.7%) (Fig.2 Bottom-right).

PC3 anchored onto the left hemisphere including temporal pole, superior temporal gyrus, middle temporal gyrus and angular gyrus (Fig.2 Top-right) and was named as the left temporal module. PC3 displayed a unique developmental signature, making a significant positive contribution to the emotion generation effect during two distinct developmental phases: late childhood (9.26–11.5 years) and late adolescence (15.5–17.26 years) (Fig.2 Top-left). The activation of PC3 was larger than PC2 at ages 8 and 15 (Fig.2 Bottom-left). PC3 was similarly lateralized to the left DMN (61.9%), Limbic (19.6%), and VAN (13.5%) (Fig.2 Bottom-right).

PC4 anchored onto the right OFC, middle temporal gyrus, temporal pole and supramarginal gyrus (Fig.2 Top-right) and was named as the right frontotemporal module. PC4 demonstrated a specific developmental sensitivity, making a significant positive contribution to the emotion generation effect exclusively during early-to-mid adolescence (12–15.5 years) (Fig.2 Top-left). And the activation of PC4 was the largest among the PCs in all sliding windows and peaked at ages 12 and 17 (Fig.2 Bottom-left). PC4 was exclusively restricted to the right DMN (74.9%) and right VAN (12.2%) (Fig.2 Bottom-right).

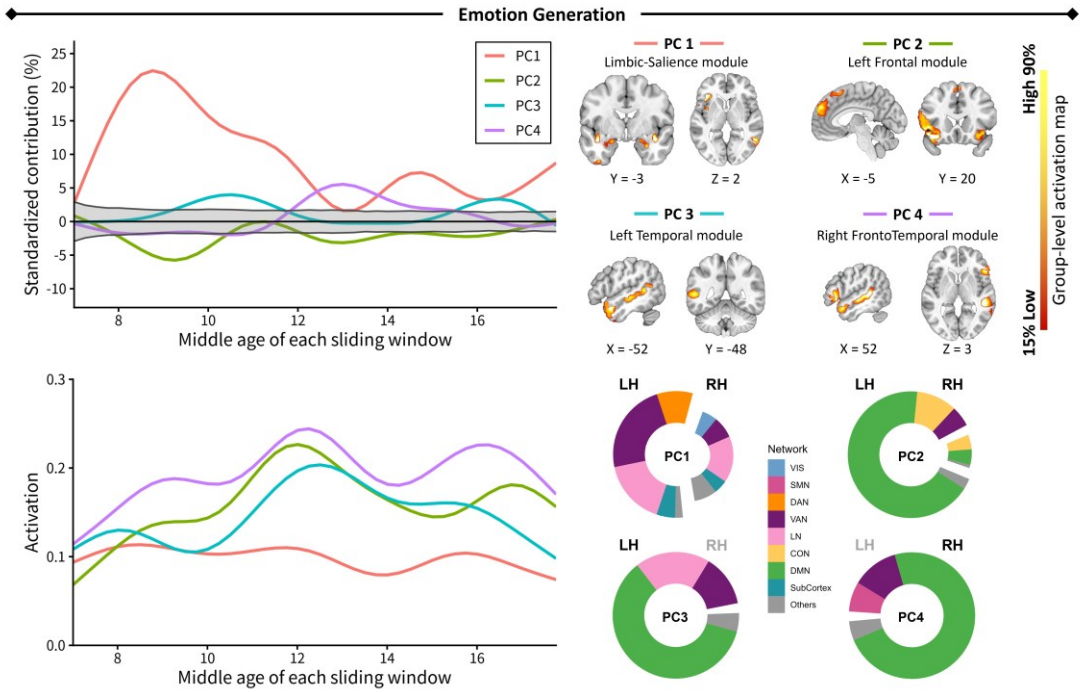


Fig. 2 Developmental trajectories of neural contributions to emotion generation. Top-left: Age-related developmental changes in the contribution of neural modules to the emotion generation effect. The x-axis represents the midpoint age of each sliding window. The y-axis represents the standardized contribution (%) of each PC. The gray shaded area represents the significance threshold, and curves extending beyond this area indicate statistically significant contributions. FD, MRI scanner model and gender were included as covariates in the model. **Top-right:** Spatial topography of the corresponding PCs. The brain maps display the spatial distribution of each module, with colors indicating relative intensity based on the group-level activation map. **Bottom-left:** Longitudinal changes in the mean activation of the neural modules. The x-axis represents the midpoint age of each sliding window. **Bottom-right:** Pie charts show the percentage of cortical voxels from the corresponding maps located in each of the seven resting-state cortical networks from Yeo[21]. The left arc represents the left hemisphere. The right arc represents the right hemisphere.

Contribution of three PCs to emotion regulation across development

Turning to the emotion regulation phase, the neural activation patterns were optimally decomposed into three distinct components. PC1 anchored onto the left dlPFC, middle temporal gyrus, angular gyrus and lateral occipital cortex (Fig.3 Top-right and Supplementary Table 4) and was named as the left frontotemporal module. PC1 demonstrated a specific early-childhood sensitivity, making a significant negative contribution to the emotion regulation effect exclusively during the 7.5- to 9-year-old window (Fig.3 Top-left). The activation of this component progressively increased across all sliding windows (Fig.3 Bottom-left and Supplementary Table 3). The module demonstrated a remarkably cohesive topology, being almost entirely confined to the left DMN (93.5%) (Fig.3 Bottom-right).

PC2 anchored onto the bilateral temporal pole, superior temporal gyrus, middle temporal gyrus and angular cortex (Fig.3 Top-right) and was named as the bilateral temporal module. PC2 exhibited a distinct multi-phase developmental signature, exerting a significant positive contribution to the emotion regulation effect across three specific windows: early childhood (7–9.76 years), early adolescence (11.76–13.76 years), and late adolescence (15.76–17.76 years) (Fig.3 Top-left). The activation of PC2 was lower than that of PC1 and PC3 from age 8 onward (Fig.3 Bottom-left and Supplementary Table 5). PC2 also mapped preferentially to the left DMN (48.5%), with additional involvement of the limbic network (10.8%) (Fig.3 Bottom-right).

Finally, PC3 anchored onto the bilateral lateral occipital cortex (Fig.3 Top-right) and was named as the bilateral occipital module. PC3 demonstrated a remarkably stable developmental profile, exerting a significant negative contribution to the emotion regulation effect across nearly the entire developmental spectrum (Fig.3 Top-left). A transient loss of significance occurred only between 10.5 and 11 years. The activation of PC3 was the largest among all PCs from 7 to 11 years, but fell below that of PC1 from age 12 onward (Fig.3 Bottom-left). This module revealed a more sensory-attention topography, characterized by dominant engagement of the visual network (35.0%) and DMN (20.3%) in the right hemisphere, as well as the dorsal attention network (DAN) (13.5%) in the left hemisphere (Fig.3 Bottom-right).

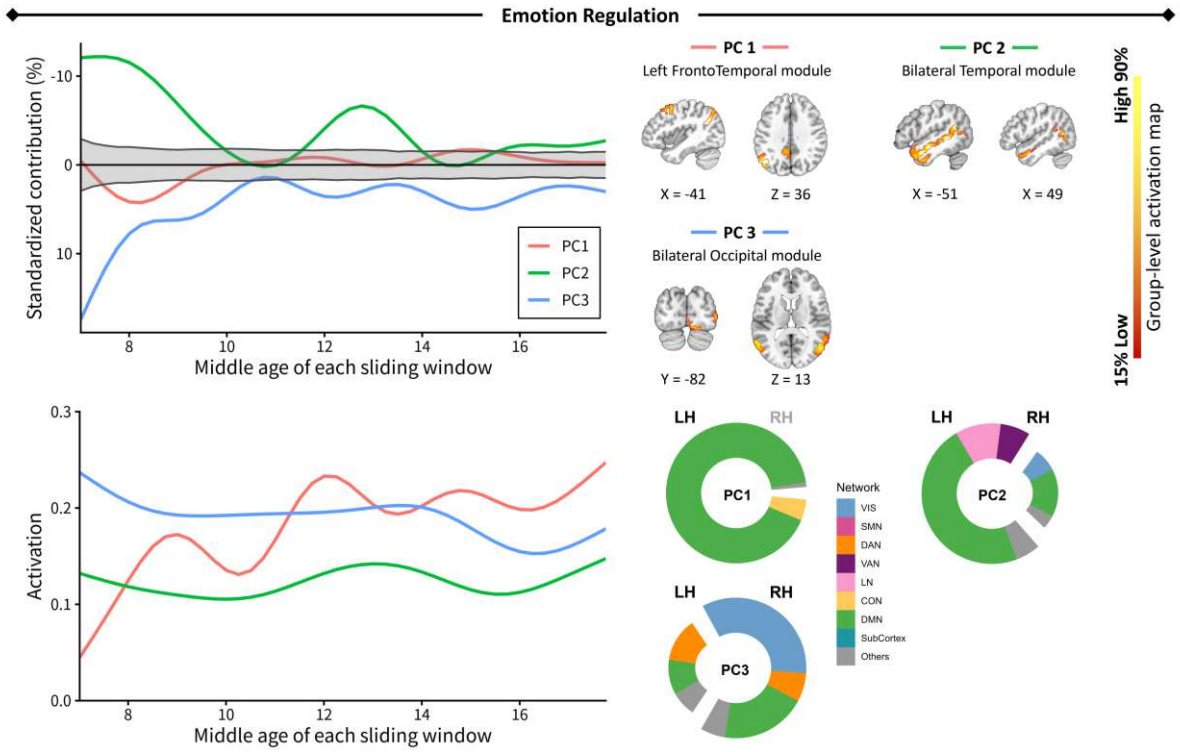


Fig. 3 Developmental trajectories of neural contributions to emotion regulation. Top-left: Longitudinal changes in the contribution of neural modules to the emotion regulation effect. The x-axis represents the midpoint age of each sliding window. The y-axis represents the standardized contribution (%) of each PC. The gray shaded area represents the significance threshold, and curves extending beyond this area indicate statistically significant contributions. FD, MRI scanner model and gender were included as covariates in the model. **Top-right:** Spatial topography of the corresponding PCs. The brain maps display the spatial distribution of each module, with colors indicating relative intensity based on the group-level activation map. **Bottom-left:** Longitudinal changes in the mean activation of the neural modules. The x-axis represents the midpoint age of each sliding window. **Bottom-right:** Pie charts show the percentage of cortical voxels from corresponding maps located in each of the seven resting-state cortical networks from Yeo[21]. The left arc represents the left hemisphere. The right arc represents the right hemisphere.

To examine cross-process coupling between the activation patterns of emotion generation and regulation, we quantified the correlations between the contributions of their respective modules. We observed a significant positive correlation between Regulation PC1 and Generation PC1 (r = 0.52, p < 0.001). Conversely, significant negative coupling emerged between Regulation PC1 and Generation PC4 (r = -0.42, p = 0.004), as well as between Regulation PC3 and Generation PC3 (r = -0.31, p = 0.04). Correlation analyses involving the deactivation modules of emotion generation are detailed in the Supplementary Materials (Supplementary Fig. 9).

Functional annotation of the PCs

To delineate the functional significance of the identified neural modes, we performed a quantitative

decoding analysis using 50 psychological topic maps related to mental processes—for example, face processing, inhibition and reward from https://neurosynth.org/. We calculated the spatial correlations between the maps of each PC and the reverse-inference maps associated with psychological functions (Fig. 4 and Supplementary Table 8-9).

During the emotion generation phase (Fig. 4a), the dominant component (PC1) exhibited robust spatial correlations with affective and clinically relevant topics, specifically "depression" (r = 0.53), "fear" (r = 0.48), and "stress" (r = 0.47), suggesting a primary role in negative affect processing. In contrast, PC2 and PC3 were functionally distinct, showing associations with higher-order cognitive and linguistic processes, such as "verbs" (r = 0.56 for PC2), "reasoning" (r = 0.49 for PC2), and "sentences" (r = 0.48 for PC3). PC4 appeared to capture sensory-social integration, correlating with "hearing" (r = 0.33) and "social" (r = 0.30).

The emotion regulation phase (Fig. 4b) revealed a shift in functional architecture. PC1 and PC2 were primarily characterized by cognitive and syntactic terms (e.g., "sentences", "reasoning", "verbs"), consistent with the recruitment of cognitive control and narrative processes during regulation. Notably, PC3 in the regulation phase displayed a distinct somatosensory profile, showing strong convergence with "body" (r = 0.53) and "motion" (r = 0.42), highlighting the involvement of embodied and sensorimotor systems in the regulatory process.

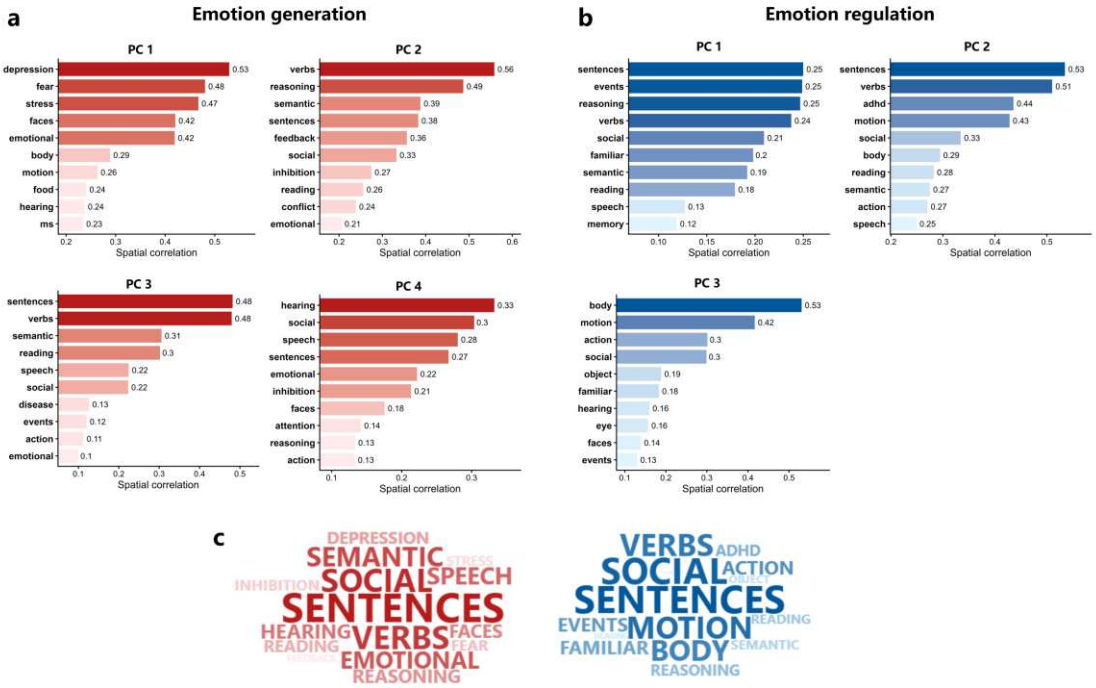


Fig. 4 Function annotation using Neurosynth topic maps. a & b: Spatial correlation between neural modules and Neurosynth topics. **c:** Word cloud of the main related topics of generation and regulation neural modules.

Relation between activation of the PCs and other emotion-related measures

We examined the linear and quadratic associations between activation of the PCs during the emotion generation and regulation phases and a range of external emotion-related measures. Associations involving the deactivation modules of emotion generation are detailed in the Supplementary Materials (Supplementary Fig. 10). All reported associations are statistically significant. Comprehensive statistical parameters are detailed in Supplementary Table 10.

During emotion generation, PC1 exhibited a specific profile linked to emotion recognition and social difficulties. Specifically, PC1 showed a significant positive linear association with the happy threshold (i.e., the emotion intensity necessary for recognizing happy faces) and social problems (Fig. 5a). Furthermore, this module demonstrated significant inverted U-shaped relations with both emotion and self-esteem responses in the non-social negative condition of the cake task. Specifically, medium PC1 activation levels corresponded to heightened sensitivity to non-social negative feedback (Fig. 5b, c). The activation of PC2 showed a negative linear association with thought problems (Fig. 5a), alongside U-shaped associations with angry RT (i.e., the reaction time to

accurately recognize angry faces above the threshold) and cognitive reappraisal (Fig. 5b, c). Specifically, extreme PC2 activation levels were associated with slower angry recognition and greater use of cognitive reappraisal for emotion regulation. PC3 emerged as a multidimensional marker of emotional sensitivity and psychopathology. Linearly, its activation was associated with enhanced processing of positive social cue evidenced by a negative relationship with the happy threshold and positive relationships with positive emotion and self-esteem increase across both social and non-social positive contexts of the cake task (Fig. 5a). However, this heightened sensitivity was accompanied by broader maladjustment, showing positive linear associations with daily negative emotion, reactive aggression, internalizing problems, and withdrawn/depression. Quadratically, PC3 displayed U-shaped relations with expression suppression and depression, while showing an inverted U-shaped relation with social problems (Fig. 5b, c). Finally, PC4 was positively linearly associated with self-esteem decrease in response to the non-social negative condition of the cake task (Fig. 5a) and exhibited inverted U-shaped associations with both anxiety and depression, where extreme activation levels corresponded to low symptom severity (Fig. 5b, c).

As to emotion regulation, PC1 was positively linearly associated with daily negative emotion (Fig. 5a). Quadratically, it showed inverted U-shaped relations with internalizing problems and self-esteem decrease in social negative feedback condition (Fig. 5b, c). Notably, PC2 was indicative of a resilient or adaptive regulatory phenotype, demonstrating negative linear associations with anxiety, depression, and daily negative emotion (Fig. 5a). This module also exhibited quadratic relations, including U-shaped associations with happy RT and angry RT, and inverted U-shaped associations with attention and social problems (Fig. 5b, c). Lastly, PC3 only displayed a U-shaped association with the use of expression suppression and self-esteem decrease in social negative feedback condition (Fig. 5b, c).

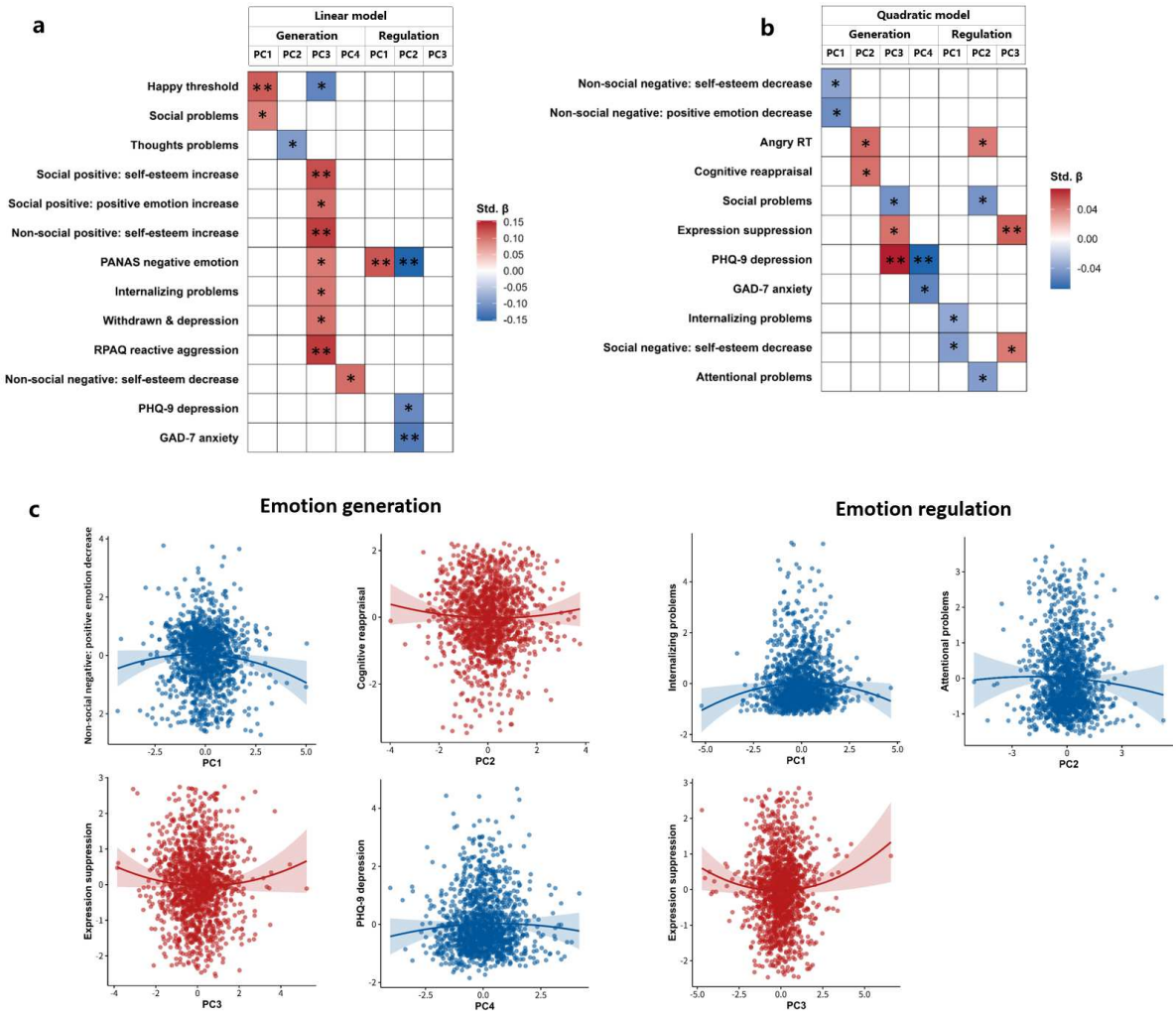


Fig. 5 Linear and quadratic relations between activation of the neural modules and other emotion-related measures. a & b : For each external emotion-related measure, all PCs derived from a given phase were simultaneously included in the regression model to isolate the unique contribution of each neural module. FD, MRI scanner model and gender were included as covariates. Blue or red color represented the significant positive or negative standardized β value of the linear or quadratic term. The white color denotes the nonsignificant relations. * $p < 0.05$, ** $p < 0.01$. **c:** Scatterplots between activation of the neural modules and other emotion-related measures. Red color represented the U-shape relationship, and blue color represented the inverted U-shape relationship. Both dependent and independent variables in the scatterplots were standardized.

Discussion

Prevailing neural developmental accounts of emotion have often framed maturation as primarily a progressive strengthening of prefrontal "top–down" control over subcortical affective responses. While this perspective captures important endpoints of adult emotion regulation, it does not fully explain how the brain's functional architecture reorganizes across childhood and adolescence, and

why development is frequently non-linear and stage-dependent[22,23]. Using a large cross-sectional sample spanning ages 6–19 and a sliding-window approach, we went beyond mere activation magnitudes to estimate age-varying contributions of the task-derived neural modules to emotion generation and regulation. This approach revealed divergent developmental trajectories of contribution versus activation of the neural modules. Together, the results suggest that emotional maturation reflects shifting weights among distributed modules rather than a monotonic increase of prefrontal control[24,25].

The activation pattern of emotion generation consists of four neural modules: (1) the limbic-salience module, (2) the left frontal module, (3) the left temporal module, and (4) the right frontotemporal module. The developmental trajectories of these modules' activation reveal a clear "visceral-to-conceptual" ontogenetic shift[10,24,26]. While the overall activation of the limbic-salience module remains low and stable, the activation profiles become overwhelmingly dominated by DMN-anchored cortical modules during late childhood and adolescence. This increasing recruitment of higher-order functional networks suggests that as the developing brain matures, emotion generation increasingly involves abstract, conceptual processes rather than purely visceral responses[27–32]. The DMN is fundamentally implicated in self-referential processing, mentalizing, and the semantic construction of emotion[33–38]. Thus, the surging activation in the left- and right-lateralized frontal and temporal neural modules likely reflects adolescents' growing neural recruitment to integrate social contexts, autobiographical memory, and complex situational appraisals into their emotional generation process[39–41].

However, from the perspective of contribution, the limbic-salience module acts as the foundational backbone of negative emotion generation. Because rapid salience detection is evolutionarily conserved and essential for basic survival, this bottom-up visceral alarm system must remain continuously engaged[42,43]. Our meta-analytic decoding further substantiates this fundamental role, revealing that this module spatially correlates with affective and clinically relevant topics, specifically "depression", "fear" and "stress", underscoring its primary function in negative affect processing. In contrast, the contribution of the left temporal and right frontotemporal modules vary inversely and alternately from age 9 onward. This non-linear trajectory suggests a developmental hand-off between competing cognitive strategies for emotion construction. The left

temporal module is classically associated with language-mediated conceptualization, semantic retrieval, and internal narrative[44,45]. Consistent with this functional profile, our meta-analysis demonstrated that this module is preferentially associated with higher-order cognitive and linguistic processes, notably “reasoning” and “semantic” processes. The right frontotemporal network is preferentially tuned to non-verbal social cues, visuospatial context, and interpersonal monitoring[46]. The localization aligns with our meta-analytic results, which show correlations with sensory-social terms like “hearing” and “social”. As children transition into preadolescence, a period marked by rapidly increasing social complexity, their developing brains may alternate between these two distinct modes of emotional meaning-making[40,47]. Additionally, the left frontal module (including left dmPFC, left OFC and bilateral p-insular cortex) showed a negative contribution to negative emotion generation from age 8 onward. It is possible that the frontal network participates in the implicit regulation during emotion generation[11,48–50]. This top-down regulatory role is further supported by the meta-analytic findings, which linked this module to abstract linguistic and action-oriented processes, such as “verbs” and “reasoning”.

During the emotion regulation phase, neural activation was optimally decomposed into three distinct modules: (1) the left frontotemporal module, (2) the bilateral temporal module, and (3) the bilateral occipital module. The increasing activation of the left frontotemporal module across development. aligns with established developmental models of emotion regulation, which posit a gradual maturation and strengthening of top-down prefrontal inhibitory systems across childhood and adolescence[51,52]. Furthermore, the co-activation of left frontal and temporal regions suggests a qualitative shift in regulatory strategies. Because the left frontotemporal network is densely involved in language processing and semantic retrieval, its increasing engagement likely reflects older adolescents' growing utilization of language-mediated, cognitively demanding strategies, such as internal self-talk, semantic reframing, and explicit cognitive reappraisal to actively modulate their affective states[53,54]. Meanwhile, the relative stability of the other two modules’ activation implies that basic visual and general temporal processing during regulation mature earlier and remain relatively stable thereafter.

Turning from activation to contribution, our findings reveal a pattern inconsistent with traditional prefrontal-centric models of emotion regulation. The bilateral temporal module emerged

as the sole positive contributor to regulation performance. Our meta-analytic decoding revealed that this module is heavily characterized by cognitive and syntactic terms such as “sentences”, “reasoning”, and “verbs”. For children and adolescents, the ability to construct a coherent semantic context or internal narrative may be a highly accessible and effective strategy for down-regulating negative affect, serving as a reliable regulatory mechanism while prefrontal executive functions are still maturing.

Conversely, activation of the left frontotemporal module exhibited a negative relation with regulation performance at age 8. Drawing on the neural efficiency hypothesis, this early negative association may reflect compensatory effort or neural inefficiency[55–57]. At age 8, children may exert immense cognitive effort to recruit this prefrontal-anchored control network. Yet, due to its immaturity, this hyperactivation fails to support effective regulation and may instead reflect a burdensome, inefficient cognitive load that interferes with regulation performance.

Furthermore, the prominent reliance on semantic-temporal networks, rather than classical prefrontal control regions, may reflect culturally specific neural cognitive strategies. Given that our sample comprises exclusively Chinese participants, this pattern aligns with cross-cultural neuroimaging evidence. East Asian cultures often emphasize interpersonal harmony and context-dependent emotional modulation, tending to value implicit regulation or contextual reappraisal over explicit top-down cognitive control[58–60]. Thus, the temporal lobe's capacity for contextual and semantic integration might be uniquely prioritized in this cultural setting. Future cross-cultural studies are necessary to determine the generalization of these modular contributions.

Finally, the bilateral occipital module contributed negatively to regulation performance across nearly all ages. This finding is highly consistent with a recent fMRI study in adults, which also demonstrated that occipital activation inversely predicts regulation performance[49]. Based on our meta-analytic results and previous literature, the regions comprising this module are classically associated with basic vision, motion perception, and visual attention[61]. The visual sensation network plays an important role in emotion regulation, but its sustained or heightened activation may be detrimental to effective regulation[62–66]. This negative association can be explained through the lens of attention deployment[67]. Effective emotion regulation, whether through distraction or cognitive reappraisal, often requires children and adolescents to shift their visual and cognitive focus away

from the salient emotional features of a stimulus toward its non-emotional or neutral contextual elements. Successful execution of this strategy naturally leads to down-regulation of activity in the primary visual cortex processing the distressing cue[68,69]. Consequently, persistent hyper-activation in the bilateral occipital module may reflect a failure to visually disengage from the emotional trigger. In other words, individuals whose visual cortices remain highly active may be attentionally "stuck" on the negative stimuli, thereby compromising their overall regulatory performance.

Beyond analyzing emotion generation and regulation separately, we conducted coupling analyses to reveal how neural modules supporting the two processes coordinate across development. First, we observed a strong positive correlation between the contributions of the limbic-salience module in emotion generation and the left frontotemporal module in emotion regulation. This may reflect a reactive or compensatory neural mechanism. Specifically, when children and adolescents rely heavily on the bottom-up, visceral alarm system for the generation of negative affect, they tend to experience greater emotional burden, which in turn requires a stronger recruitment of top-down, language-mediated control networks to manage the distress[9,70]. Conversely, significant negative coupling emerged between the right frontotemporal module in emotion generation and the left frontotemporal module in emotion regulation. This inverse association may reflect a strategic or hemispheric trade-off in emotion processing[71,72]. When emotional meaning is primarily derived from external, non-verbal social cues and visuospatial contexts (right-lateralized), the developing brain may rely less on internal semantic reframing and language-based narrative processes (left-lateralized) for regulation. This indicates that children and adolescents might implicitly adopt regulatory strategies that align with their mode of emotional appraisal. Finally, the negative association between the left temporal module in emotion generation and the bilateral occipital module in emotion regulation highlights a fascinating dichotomy between internal and external processing orientations. As discussed previously, the left temporal module is strongly associated with internal semantic conceptualization, whereas the bilateral occipital module is linked to visual processing and attention deployment. This negative coupling implies that when children and adolescents tend to construct emotions through deep internal narratives and semantic retrieval, they are less likely to employ external visual disengagement (e.g., simply looking away from the stimulus) as a regulatory strategy[67,73]. Together, these cross-process couplings underscore that emotional

maturation reflects not merely the development of isolated regions, but developmentally shaped coordination of the distributed, brain-wide neural modules that support the alignment between appraisal processes and regulatory strategies.

Having established the dynamic developmental patterns of these emotion generation and regulation modules, a critical next step is to understand how individual differences in activation of these neural modules relate to other emotion processes and real-world psychological well-being. Consistent with their task-derived contributions, the linear associations between modular activation and external measures clearly distinguish adaptive phenotypes from those conferring affective vulnerability. Specifically, the left frontal module involved in emotion generation and the bilateral temporal module supporting emotion regulation both emerged as neurocognitive buffers that protect against psychological distress. The left frontal module, which we identified as implicitly down-regulating negative emotion during generation, was linearly associated with fewer thought problems. Similarly, the bilateral temporal module, the sole positive contributor to regulation performance, exhibited strong negative linear associations with anxiety, depression, and daily negative emotion. Together, these findings corroborate our behavioral results, suggesting that individuals who can efficiently recruit these frontal and temporal networks possess a more adaptive regulatory phenotype, enabling them to better mitigate emotional disturbances in daily life[74,75].

Conversely, modules associated with the bottom-up generation of negative affect or inefficient regulation predicted poorer psychological adjustment. The limbic-salience module in generation and the left frontotemporal module in regulation were both linearly associated with heightened emotional difficulties. The limbic-salience module activation was linked to a higher threshold for recognizing happy expression and increased social problems, while the left frontotemporal module was linked to higher daily negative emotion. This pattern implies that an over-reliance on the visceral alarm system, or the inefficient, perhaps excessively demanding recruitment of left frontotemporal regions during regulation, may index a vulnerability to emotional and social maladjustment[76,77].

Perhaps most intriguingly, the left temporal module in emotion generation emerged as a complex, double-edged marker of emotional hypersensitivity. Linearly, higher activation in this semantic and narrative-related module predicted enhanced processing of positive cues, including

lower recognition thresholds for happy expression and greater emotion and self-esteem increase after positive feedback. However, this module was simultaneously linked to broader maladjustment, including daily negative emotion, reactive aggression, and internalizing symptoms. We propose that high activation of the left temporal module may reflect an "emotional hyper-conceptualization" phenotype. As children and adolescents increasingly rely on language and internal narratives to construct emotions, those who over-engage this left temporal network may experience affective cues more vividly[28,78]. While this intense semantic elaboration allows for rich positive emotional experiences, it may also predispose individuals to maladaptive cognitive tendencies such as rumination or exaggerated interpretation of negative social cues, thereby increasing the risk of internalizing and aggressive symptoms[79,80].

Beyond these linear relations, our analysis revealed widespread quadratic associations for both emotion generation and regulation modules. Some quadratic results reveal that optimal emotional functioning likely requires a homeostatic balance[81–84]. For instance, extreme activation of modules like the left temporal module involved in emotion generation and the bilateral occipital module involved in emotion regulation were both linked to greater use of expression suppression. Conversely, intermediate activation of the left frontal module in emotion generation and the bilateral temporal module in emotion regulation were related to less use of cognitive reappraisal and higher attention problems. The inverted associations may capture a vulnerable state of neural inefficiency or strategic conflict[85,86]. Children and adolescents may exert enough cognitive effort to experience mental fatigue, yet fail to recruit these target networks robustly enough to achieve successful emotional resolution. This incomplete engagement leaves them in a state of high cognitive load but low regulatory reward, thereby maximizing affective distress.

Finally, these findings must be interpreted in light of methodological constraints. First, our analytical framework employed PCA to identify functional modules based on spatial co-activation. While this effectively captures macroscopic activation patterns, PCA inherently groups regions that co-activate without considering their independent contributions to behavior. As a result, spatial co-activation may obscure behavioral heterogeneity, such that distinct sub-regions within a single module could exert divergent, or even opposing, effects on emotion generation or regulation performance[87,88]. Second, the observed quadratic relationships between neural activation and

psychological measures must be interpreted cautiously. Non-linear polynomial models can be disproportionately sensitive to extreme values at the tails of a distribution. Although some of these trajectories align well with neural developmental theories of homeostatic balance and neural inefficiency, further replication in independent, preferably longitudinal, cohorts are necessary to confirm that these non-linear patterns are robust and not driven by statistical artifacts.

In summary, this study provides a dynamic functional architecture of emotional neural development. By disentangling neural activation magnitudes from their contributions to emotion generation and regulation, and charting their developmental trajectories using a sliding-window approach, we reveal that emotional maturation is not a monotonic strengthening of prefrontal control. Rather, it is a complex, non-linear reorganization shifting from visceral, bottom-up processing toward a sophisticated, language-mediated conceptualization of emotion. We go beyond static snapshots to reveal a developing brain continuously negotiating between its internal physiological state and the external social environment. Our findings suggest that clinical interventions should be stage-matched: targeting somatic regulation and visual attention disengagement in childhood, while scaffolding healthy semantic interpretation and social reality-testing during the dynamic network reorganization of adolescence.

Methods

Participants and paradigm of fMRI task

A total of 1464 participants (747 males and 717 females, mean age = 13.03 ± 3.53 years) were drawn from the China Child Brain Development Project (CCBD)[89]. These participants completed an emotion regulation and trust task. During emotion regulation phase, participants viewed 6 neutral and 15 negative images from the China Face Affect Picture System (CFAPS). First, a 2.5-s cue (‘Look’ or ‘Decrease’) instructed participants to either attend to the images (‘Look’) or decrease their negative emotional responses to the aversive images by reappraising their meaning and context (‘Decrease’). The task comprised 6 ‘Look neutral’ trials, 6 ‘Look negative’ trials and 9 ‘Decrease negative’ trials. Following the cue, participants had 6s to rate their current emotion status. Subsequently, each trial concluded with a trust task phase. Participants engaged in a simulated

interpersonal interaction, receiving a monetary investment from a peer (the face they had just viewed) and were instructed to decide the amount of money to reciprocate. Given the specific focus of the current research, both the behavioral and neuroimaging data acquired during this trust phase fell outside our scope and were excluded from the analysis. The E-Prime software was used to present the overall task and collect behavioral ratings. All research materials and procedures have been approved by the Institutional Review Board of Beijing Normal University (IRB_A_0054_2023004)

fMRI data acquisition and preprocessing

The data were collected on Siemens 3T Prisma, UH uMR890 and GE MR750 scanners, including T1-weighted images and resting-stats function MRI (Supplementary Fig. 11). All preprocessing was conducted using the fMRIPrep workflow[90]. The first 10 volumes (7.5 s) of the functional imaging data were discarded as dummy scans to allow for magnetization equilibrium and participant habituation. Head motion correction was performed using the mcflirt tool from the FMRIB Software Library (FSL, https://fsl.fmrib.ox.ac.uk/), where all 3D BOLD images were rigidly registered to a single-band reference image. Susceptibility-induced distortion correction was applied using fieldmaps processed via FSL's fsl_prepare_fieldmap and fugue tools, yielding a distortion-corrected BOLD reference. The reference image was then co-registered to the participant's skull-stripped T1-weighted (T1w) structural image using boundary-based registration (BBR). Then all images were normalized to MNI152NLin2009cAsym (2.4 mm isotropic resolution) space. To minimize spatial interpolation artifacts, the affine matrices from motion correction and T1w co-registration, along with the deformation fields from distortion correction and standard space normalization, were concatenated. These combined transformations were applied in a single step to the original BOLD time series (excluding dummy scans) to normalize the images to standard volume space.

For each functional run, data were considered usable if 80% of the sequence had a framewise displacement of less than 0.9 mm. To further mitigate physiological and motion-related artifacts, nuisance signals were regressed out from the normalized BOLD data using a general linear model (GLM). Nuisance regressors included the global signal, mean white matter and cerebrospinal fluid signals, multiple components extracted via the CompCor method, and framewise displacement (FD). The regression model incorporated either the Friston-24 head motion parameters or the standard six motion parameters, along with linear and quadratic temporal trends.

After regression, the constant term of the model was added back to preserve image-to-background contrast. Subsequently, a high-pass filter (>0.0078 Hz) was applied to the time series using AFNI's 3dbandpass command to remove low-frequency temporal drift, with the temporal mean image added back post-filtering. Finally, the filtered volume and surface data were spatially smoothed using a 6-mm full-width-at-half-maximum (FWHM) Gaussian kernel via Connectome Workbench.

Neural modules identification approach

Firstly, we conducted a second level analysis using SPM12[91]. We created a gray matter mask using MNI152NLin2009cAsym space gray matter probability map (cutoff = 0.5) and resampled it to the same resolution as the previous preprocessing. Then we used a single sample t-test to determine the group activation patterns under different task contrasts (shown in Supplementary Fig. 2-4, FDR.$p <$ 0.05, cluster size > 200 voxels), and included gender, age, mean FD, and different MRI devices as covariates. Under the above statistical conditions, we obtained three significant contrast maps respectively (Activation and deactivation maps for emotion generation, and activation map for emotion regulation.).

For each contrast, we conducted PCA decomposition along the voxel dimension among the significant regions. Specifically, we obtained a matrix of *N* (participants) × n (voxels) to extract the voxel patterns of common changes across development. The optimal number of PCs is selected using the elbow method and the positive directions of all PCs are defined as the same direction as the original activation value. Spatial maps were generated by assigning each voxel to the PC with the highest positive loading, and individual PC scores were calculated, and clusters with less than 100 voxels of each PC are removed. The score of each PC is the average of the standard β value of activation corresponding to all voxels.

Dynamic-siding window approach

To quantify the dynamic contribution of these neural components to behavior, we employed a sliding window approach (window size = 2 years, step size = 0.25 years) across the full age range of the sample. Within each sliding window, multiple regression models were fitted to predict task performance (emotion generation: difference between ratings of negative affect in 'Look negative'

548 and ‘Look neutral’; emotion regulation: difference between ratings of negative affect in ‘Look
549 negative’ and ‘Regulate negative’) using activation z-scores of all corresponding PCs. The equation
550 is provided in the following:

551 $$task\ score_k \sim \beta_{k1} \cdot PC1 + \ \beta_{k2} \cdot PC2 + \cdots + \ \beta_{km} \cdot PCm + covariates$$

552 The contribution of each PC was quantified using the following formula:

553 $$contribution_{km} = \beta_{km}^2 \cdot SIGN(\beta_{km})$$

554 Here β_{km}^2 refers to the variance each PC explained (R^2). $SIGN(\beta_{km})$ refers to the sign of
555 each PC’s standardized regression coefficient.

556 **Analysis on neural module activation**

557 Participants were stratified into 2-year age bins (6-7, 8-9, ..., 18-19 years). To examine the
558 relative activation ranking of neural modules within each age group, we used linear mixed models
559 with each neural module activation as the dependent variable, age group × neural module as fixed
560 effects, and MRI equipment, gender, and mean framewise displacement as covariates. Subject ID
561 was included as a random intercept to account for the non-independence of multiple PC scores from
562 the same participant. Estimated marginal means were extracted and pairwise comparisons within
563 each age group were conducted with Tukey correction. Compact letter display was used to visualize
564 significant differences among components. To assess the linear association between age and each
565 neural module activation, we fitted separate linear models with the same covariates and applied
566 Benjamini-Hochberg false discovery rate correction across the nine dependent variables.

567 **Other emotion-related measures**

568 Among all the participants who completed fMRI task, 1396 participants (697 males and 699 females,
569 mean age = 13.07 ± 3.54 years) also completed other 8 emotion-related measures. These measures
570 were Morphed Emotion Recognition Task[92], Cake task[93], Emotion Regulation Questionnaire
571 (ERQ)[94], Generalized Anxiety Disorder (GAD)[95], Patient Health Questionnaire (PHQ)[96], Positive
572 and Negative Affect Scale (PANAS)[97], Child Behavior Checklist (CBCL)[98] and Reactive and
573 Proactive Aggression Questionnaire (RPAQ)[99]. For each emotion-related measure, all PCs derived
574 from a given phase were simultaneously included in the linear or quadratic regression model to

isolate the unique contribution of each neural module. FD, MRI scanner model and gender were included as covariates. Missing data were replaced by mean imputation.

The Morphed Emotion Recognition Task assesses individuals' ability to recognize facial emotions of varying intensities[92]. In this task, images of faces showing three types of emotion (happiness, calmness/neutrality, anger) were presented, and participants selected the corresponding cartoon expression that matches the emotion in the images. Ten intensity levels (10% to 100%) were created for happy and angry expressions by morphing them with neutral expression, resulting in 21 experimental conditions: (2 emotions × 10 intensities) + neutral emotion. Prior to the formal task, participants completed two practice sessions: (1) distinguishing the three cartoon expressions; (2) matching 100%-intensity facial images to corresponding cartoon expressions. The formal task followed the same procedure as the second practice session, but facial expression intensities (10%–100%) were randomized across trials. With 4 trials per condition, the formal task included 84 total trials. We constructed a computational model for this task to calculate the recognition thresholds for happy and angry expressions:

$$P(acc) = Probit(threshold + s * intensity)$$

$Threshold$ and s were free parameters. After each subject's thresholds for happy and angry expressions were estimated, the mean reaction times of correct trials above two emotion thresholds. For model estimation, we used the rstan package in R (https://mc-stan.org).

The cake task assessed children's and adolescents' emotion and self-esteem in response to positive and negative contexts, using a scenario in which participants make a cake and gift it to a virtual character[93]. Before the task, participants reported their current positive emotion (7-point scoring) and self-esteem (7-point scoring) to establish a baseline for subsequent index calculation. Upon the start of formal testing, participants completed two core phases: (1) a cake-making phase, in which they selected a cake base and bake the cake; (2) a gifting phase, in which they chose the cake as a gift to the virtual character. In positive contexts, participants experienced 5 successful trials, defined as completed cake-making (non-social) or receiving positive feedback from the virtual character (social), and 1 failed trial, defined as failed cake-making (non-social) or receiving negative feedback from the character (social). In the negative contexts, success-failure ratio was

reversed. After each module, participants reported their current emotion and self-esteem. The task incorporates four conditions: social vs. non-social, crossed with positive vs. negative contexts. Key dependent measures include participants' emotion ratings and self-esteem responses in four conditions with the baseline as reference. For negative contexts, we calculated baseline minus contextual scores to measure the decline in positive emotion or self-esteem. We termed this index as "social/non-social – negative: positive emotion/self-esteem decrease". For positive contexts, we calculated contextual scores minus baseline to measure the increase in positive emotion or self-esteem. We termed this index as "social/non-social – positive: positive emotion/self-esteem increase".

Neurosynth dataset

To annotate the brain function of the identified neural modules, we used the Neurosynth database (http://neurosynth.org), which relies on reported activation pattern from 11,406 studies[30]. The large scale of the Neurosynth dataset can offset potential random errors in individual studies, thereby supporting robust brain function assignment for specific regions. We selected the same 50 psychological topics as Bo et al.[49] chose. These topics were all from V4-topics-100 including face processing, inhibition and so on. Topics less related to psychological functions, such as 'stimulation', 'task' or 'paradigm', were excluded. The topic maps were computed using reverse inference, which denotes probability of the topic given activation[100]. To calculate the spatial similarity between the topic maps and the neural modules, topic maps were resampled into the same space as the neural modules. Spatial similarity was assessed via Pearson correlation between the topic maps and the neural modules in a pairwise fashion.

Data & code availability

The data and code that support the findings of this study are available from the corresponding author upon reasonable request, subject to applicable ethical and institutional data-sharing restrictions.

Acknowledgement

This work was supported by the Brain Science and Brain-like Intelligence Technology-National Science and Technology Major Project (2021ZD0200500).

Author contributions

C.Xia. and X.H. performed the analyses and prepared the figures. Q.M., X.Z., C.Xie, N.H., R.D., Y.L. and S.Q. contributed to data collection,data curation and interpretation of the results. C.Xia.drafted the manuscript. X.C. supervised the study. All authors reviewed and approved the final manuscript.

References

1. Zhou F, Zhao W, Qi Z, et al. A distributed fMRI-based signature for the subjective experience of fear. *Nat Commun*. 2021;12(1):6643. doi:10.1038/s41467-021-26977-3

2. Wilson-Mendenhall CD, Henriques A, Barsalou LW, Barrett LF. Primary Interoceptive Cortex Activity during Simulated Experiences of the Body. *J Cogn Neurosci*. 2019;31(2):221-235. doi:10.1162/jocn_a_01346

3. Camacho MC, Nielsen AN, Balser D, et al. Large-scale encoding of emotion concepts becomes increasingly similar between individuals from childhood to adolescence. *Nat Neurosci*. 2023;26(7):1256-1266. doi:10.1038/s41593-023-01358-9

4. Lettieri G, Handjaras G, Ricciardi E, et al. Emotionotopy in the human right temporo-parietal cortex. *Nat Commun*. 2019;10(1):5568. doi:10.1038/s41467-019-13599-z

5. Hoemann K, Xu F, Barrett LF. Emotion words, emotion concepts, and emotional development in children: A constructionist hypothesis. *Dev Psychol*. 2019;55(9):1830-1849. doi:10.1037/dev0000686

6. Ahmed SP, Bittencourt-Hewitt A, Sebastian CL. Neurocognitive bases of emotion regulation development in adolescence. *Dev Cogn Neurosci*. 2015;15:11-25. doi:10.1016/j.dcn.2015.07.006

7. Zhang JX, Bo K, Wager TD, Gross JJ. The brain bases of emotion generation and emotion regulation. *Trends Cogn Sci*. 2025;29(10):879-891. doi:10.1016/j.tics.2025.04.013

8. Gross JJ, Ford BQ, eds. *Handbook of Emotion Regulation*. Third edition. The Guilford Press; 2024.

9. Ochsner K, Gross J. The cognitive control of emotion. *Trends Cogn Sci*. 2005;9(5):242-249. doi:10.1016/j.tics.2005.03.010

10. Silvers JA, Insel C, Powers A, et al. The transition from childhood to adolescence is marked by a general decrease in amygdala reactivity and an affect-specific ventral-to-dorsal shift in medial prefrontal recruitment. *Dev Cogn Neurosci*. 2017;25:128-137. doi:10.1016/j.dcn.2016.06.005

11. Etkin A, Büchel C, Gross JJ. The neural bases of emotion regulation. *Nat Rev Neurosci*. 2015;16(11):693-700. doi:10.1038/nrn4044

12. Delevich K, Klinger M, Okada NJ, Wilbrecht L. Coming of age in the frontal cortex: The role of puberty in cortical maturation. *Semin Cell Dev Biol*. 2021;118:64-72. doi:10.1016/j.semcdb.2021.04.021

13. Pozzi E, Vijayakumar N, Rakesh D, Whittle S. Neural Correlates of Emotion Regulation in Adolescents and Emerging Adults: A Meta-analytic Study. *Biol Psychiatry*. 2021;89(2):194-204. doi:10.1016/j.biopsych.2020.08.006

14. Ferri J, Bress JN, Eaton NR, Proudfit GH. The Impact of Puberty and Social Anxiety on Amygdala Activation to Faces in Adolescence. *Dev Neurosci*. 2014;36(3-4):239-249. doi:10.1159/000363736

15. Gee DG, Gabard-Durnam LJ, Flannery J, et al. Early developmental emergence of human amygdala–prefrontal connectivity after maternal deprivation. *Proc Natl Acad Sci*. 2013;110(39):15638-15643. doi:10.1073/pnas.1307893110

16. Casey BJ. Beyond Simple Models of Self-Control to Circuit-Based Accounts of Adolescent Behavior. *Annu Rev Psychol*. 2015;66(1):295-319. doi:10.1146/annurev-psych-010814-015156

17. Nelson EE, Leibenluft E, McCLURE EB, Pine DS. The social re-orientation of adolescence: a

677 neuroscience perspective on the process and its relation to psychopathology. *Psychol Med*.
678 2005;35(2):163-174. doi:10.1017/S0033291704003915

679 18. Hoemann K, Wu R, LoBue V, Oakes LM, Xu F, Barrett LF. Developing an Understanding of
680 Emotion Categories: Lessons from Objects. *Trends Cogn Sci*. 2020;24(1):39-51.
681 doi:10.1016/j.tics.2019.10.010

682 19. Casey BJ, Heller AS, Gee DG, Cohen AO. Development of the emotional brain. *Neurosci Lett*.
683 2019;693:29-34. doi:10.1016/j.neulet.2017.11.055

684 20. Hayden BY, Heilbronner SR, Yoo SBM. Rethinking the centrality of brain areas in
685 understanding functional organization. *Nat Neurosci*. Published online December 23, 2025.
686 doi:10.1038/s41593-025-02166-z

687 21. Thomas Yeo BT, Krienen FM, Sepulcre J, et al. The organization of the human cerebral cortex
688 estimated by intrinsic functional connectivity. *J Neurophysiol*. 2011;106(3):1125-1165.
689 doi:10.1152/jn.00338.2011

690 22. Ahmed SP, Bittencourt-Hewitt A, Sebastian CL. Neurocognitive bases of emotion regulation
691 development in adolescence. *Dev Cogn Neurosci*. 2015;15:11-25. doi:10.1016/j.dcn.2015.07.006

692 23. Pfeifer JH, Masten CL, Moore WE, et al. Entering Adolescence: Resistance to Peer Influence,
693 Risky Behavior, and Neural Changes in Emotion Reactivity. *Neuron*. 2011;69(5):1029-1036.
694 doi:10.1016/j.neuron.2011.02.019

695 24. Silvers JA. Extinction Learning and Cognitive Reappraisal: Windows Into the
696 Neurodevelopment of Emotion Regulation. *Child Dev Perspect*. 2020;14(3):178-184.
697 doi:10.1111/cdep.12372

698 25. Vijayakumar N, Pfeifer JH, Flournoy JC, Hernandez LM, Dapretto M. Affective reactivity
699 during adolescence: Associations with age, puberty and testosterone. *Cortex*. 2019;117:336-350.
700 doi:10.1016/j.cortex.2019.04.024

701 26. Silvers JA, Insel C, Powers A, et al. vlPFC–vmPFC–Amygdala Interactions Underlie Age-
702 Related Differences in Cognitive Regulation of Emotion. *Cereb Cortex*. Published online June 23,

2016:bhw073. doi:10.1093/cercor/bhw073

27. Barrett LF, Atzil S, Bliss-Moreau E, et al. The Theory of Constructed Emotion: More Than a Feeling. *Perspect Psychol Sci*. 2025;20(3):392-420. doi:10.1177/17456916251319045

28. Barrett LF. The theory of constructed emotion: an active inference account of interoception and categorization. *Soc Cogn Affect Neurosci*. Published online October 19, 2016:nsw154. doi:10.1093/scan/nsw154

29. Critchley HD, Nagai Y. How Emotions Are Shaped by Bodily States. *Emot Rev*. 2012;4(2):163-168. doi:10.1177/1754073911430132

30. Murphy J, Brewer R, Catmur C, Bird G. Interoception and psychopathology: A developmental neuroscience perspective. *Dev Cogn Neurosci*. 2017;23:45-56. doi:10.1016/j.dcn.2016.12.006

31. MacCormack JK, Lindquist KA. Bodily Contributions to Emotion: Schachter's Legacy for a Psychological Constructionist View on Emotion. *Emot Rev*. 2017;9(1):36-45. doi:10.1177/1754073916639664

32. Supekar K, Uddin LQ, Prater K, Amin H, Greicius MD, Menon V. Development of functional and structural connectivity within the default mode network in young children. *NeuroImage*. 2010;52(1):290-301. doi:10.1016/j.neuroimage.2010.04.009

33. Huth AG, Nishimoto S, Vu AT, Gallant JL. A Continuous Semantic Space Describes the Representation of Thousands of Object and Action Categories across the Human Brain. *Neuron*. 2012;76(6):1210-1224. doi:10.1016/j.neuron.2012.10.014

34. Satpute AB, Lindquist KA. The Default Mode Network's Role in Discrete Emotion. *Trends Cogn Sci*. 2019;23(10):851-864. doi:10.1016/j.tics.2019.07.003

35. Catani M, Dell'Acqua F, Thiebaut De Schotten M. A revised limbic system model for memory, emotion and behaviour. *Neurosci Biobehav Rev*. 2013;37(8):1724-1737. doi:10.1016/j.neubiorev.2013.07.001

36. Andrews-Hanna JR. The Brain's Default Network and Its Adaptive Role in Internal Mentation. *The Neuroscientist*. 2012;18(3):251-270. doi:10.1177/1073858411403316

729 37. Spreng RN, Mar RA, Kim ASN. The Common Neural Basis of Autobiographical Memory,
730 Prospection, Navigation, Theory of Mind, and the Default Mode: A Quantitative Meta-analysis. *J*
731 *Cogn Neurosci*. 2009;21(3):489-510. doi:10.1162/jocn.2008.21029

732 38. Menon V. 20 years of the default mode network: A review and synthesis. *Neuron*.
733 2023;111(16):2469-2487. doi:10.1016/j.neuron.2023.04.023

734 39. Blakemore SJ. The social brain in adolescence. *Nat Rev Neurosci*. 2008;9(4):267-277.
735 doi:10.1038/nrn2353

736 40. Crone EA, Dahl RE. Understanding adolescence as a period of social–affective engagement
737 and goal flexibility. *Nat Rev Neurosci*. 2012;13(9):636-650. doi:10.1038/nrn3313

738 41. Fombouchet Y, Pineau S, Perchec C, Lucenet J, Lannegrand L. The development of emotion
739 regulation in adolescence: What do we know and where to go next? *Soc Dev*. 2023;32(4):1227-1242.
740 doi:10.1111/sode.12684

741 42. LeDoux J. Rethinking the Emotional Brain. *Neuron*. 2012;73(4):653-676.
742 doi:10.1016/j.neuron.2012.02.004

743 43. Ptak R. The Frontoparietal Attention Network of the Human Brain: Action, Saliency, and a
744 Priority Map of the Environment. *The Neuroscientist*. 2012;18(5):502-515.
745 doi:10.1177/1073858411409051

746 44. Binder JR, Desai RH, Graves WW, Conant LL. Where Is the Semantic System? A Critical
747 Review and Meta-Analysis of 120 Functional Neuroimaging Studies. *Cereb Cortex*.
748 2009;19(12):2767-2796. doi:10.1093/cercor/bhp055

749 45. Wagley N, Booth JR. Neuro-cognitive development of semantic and syntactic bootstrapping
750 in 6- to 7.5-year-old children. *NeuroImage*. 2021;241:118416.
751 doi:10.1016/j.neuroimage.2021.118416

752 46. Decety J, Lamm C. The Role of the Right Temporoparietal Junction in Social Interaction: How
753 Low-Level Computational Processes Contribute to Meta-Cognition. *The Neuroscientist*.
754 2007;13(6):580-593. doi:10.1177/1073858407304654

47. Pfeifer JH, Blakemore SJ. Adolescent social cognitive and affective neuroscience: past, present, and future. *Soc Cogn Affect Neurosci*. 2012;7(1):1-10. doi:10.1093/scan/nsr099

48. Kalisch R, Gerlicher AMV. Making a mountain out of a molehill: On the role of the rostral dorsal anterior cingulate and dorsomedial prefrontal cortex in conscious threat appraisal, catastrophizing, and worrying. *Neurosci Biobehav Rev*. 2014;42:1-8. doi:10.1016/j.neubiorev.2014.02.002

49. Bo K, Kraynak TE, Kwon M, Sun M, Gianaros PJ, Wager TD. A systems identification approach using Bayes factors to deconstruct the brain bases of emotion regulation. *Nat Neurosci*. 2024;27(5):975-987. doi:10.1038/s41593-024-01605-7

50. (Bud) Craig AD. How do you feel — now? The anterior insula and human awareness. *Nat Rev Neurosci*. 2009;10(1):59-70. doi:10.1038/nrn2555

51. McRae K, Gross JJ, Weber J, et al. The development of emotion regulation: an fMRI study of cognitive reappraisal in children, adolescents and young adults. *Soc Cogn Affect Neurosci*. 2012;7(1):11-22. doi:10.1093/scan/nsr093

52. Ochsner KN, Silvers JA, Buhle JT. Functional imaging studies of emotion regulation: a synthetic review and evolving model of the cognitive control of emotion. *Ann N Y Acad Sci*. 2012;1251(1). doi:10.1111/j.1749-6632.2012.06751.x

53. Buhle JT, Silvers JA, Wager TD, et al. Cognitive Reappraisal of Emotion: A Meta-Analysis of Human Neuroimaging Studies. *Cereb Cortex*. 2014;24(11):2981-2990. doi:10.1093/cercor/bht154

54. McRae K, Hughes B, Chopra S, Gabrieli JDE, Gross JJ, Ochsner KN. The Neural Bases of Distraction and Reappraisal. *J Cogn Neurosci*. 2010;22(2):248-262. doi:10.1162/jocn.2009.21243

55. Luna B. Developmental Changes in Cognitive Control through Adolescence. In: *Advances in Child Development and Behavior*. Vol 37. Elsevier; 2009:233-278. doi:10.1016/S0065-2407(09)03706-9

56. Luna B, Marek S, Larsen B, Tervo-Clemmens B, Chahal R. An Integrative Model of the Maturation of Cognitive Control. *Annu Rev Neurosci*. 2015;38(1):151-170. doi:10.1146/annurev-

781 neuro-071714-034054

782 57. Steinbeis N. A Rational Account of Cognitive Control Development in Childhood. *Annu Rev*
783 *Dev Psychol*. 2023;5(1):217-238. doi:10.1146/annurev-devpsych-120221-040058

784 58. Murata A, Moser JS, Kitayama S. Culture shapes electrocortical responses during emotion
785 suppression. *Soc Cogn Affect Neurosci*. 2013;8(5):595-601. doi:10.1093/scan/nss036

786 59. Vu TT, Vu D, Nguyen TML, eds. *Emotions in Cross-Cultural Psychology: A Curated*
787 *Literature Overview*. Springer Nature Switzerland; 2025. doi:10.1007/978-3-032-08927-4

788 60. Zhu Y, Zhang L, Fan J, Han S. Neural basis of cultural influence on self-representation.
789 *NeuroImage*. 2007;34(3):1310-1316. doi:10.1016/j.neuroimage.2006.08.047

790 61. Corbetta M, Shulman GL. Control of goal-directed and stimulus-driven attention in the brain.
791 *Nat Rev Neurosci*. 2002;3(3):201-215. doi:10.1038/nrn755

792 62. Rodriguez M, Kross E. Sensory emotion regulation. *Trends Cogn Sci*. 2023;27(4):379-390.
793 doi:10.1016/j.tics.2023.01.008

794 63. Ferri J, Schmidt J, Hajcak G, Canli T. Neural correlates of attentional deployment within
795 unpleasant pictures. *NeuroImage*. 2013;70:268-277. doi:10.1016/j.neuroimage.2012.12.030

796 64. Christou AI, Bacopoulou F. Emotion and Feeling in Parent–Child Dyads: Neurocognitive and
797 Psychophysiological Pathways of Development. *Children*. 2025;12(11):1478.
798 doi:10.3390/children12111478

799 65. Kravitz DJ, Saleem KS, Baker CI, Ungerleider LG, Mishkin M. The ventral visual pathway:
800 an expanded neural framework for the processing of object quality. *Trends Cogn Sci*. 2013;17(1):26-
801 49. doi:10.1016/j.tics.2012.10.011

802 66. Kragel PA, Reddan MC, LaBar KS, Wager TD. Emotion schemas are embedded in the human
803 visual system. *Sci Adv*.

804 67. Gross JJ. Emotion Regulation: Current Status and Future Prospects. *Psychol Inq*. 2015;26(1):1-
805 26. doi:10.1080/1047840X.2014.940781

806 68. Ferri J, Hajcak G. Neural mechanisms associated with reappraisal and attentional deployment.
807 *Curr Opin Psychol*. 2015;3:17-21. doi:10.1016/j.copsyc.2015.01.010

808 69. Ferri J, Schmidt J, Hajcak G, Canli T. Emotion regulation and amygdala-precuneus
809 connectivity: Focusing on attentional deployment. *Cogn Affect Behav Neurosci*. 2016;16(6):991-
810 1002. doi:10.3758/s13415-016-0447-y

811 70. Banks SJ, Eddy KT, Angstadt M, Nathan PJ, Phan KL. Amygdala–frontal connectivity during
812 emotion regulation. *Soc Cogn Affect Neurosci*. 2007;2(4):303-312. doi:10.1093/scan/nsm029

813 71. Van Der Knaap LJ, Van Der Ham IJM. How does the corpus callosum mediate
814 interhemispheric transfer? A review. *Behav Brain Res*. 2011;223(1):211-221.
815 doi:10.1016/j.bbr.2011.04.018

816 72. Helmstaedter C, Kurthen M, Lux S, Reuber M, Elger CE. Chronic epilepsy and cognition: A
817 longitudinal study in temporal lobe epilepsy. *Ann Neurol*. 2003;54(4):425-432.
818 doi:10.1002/ana.10692

819 73. Chun MM, Golomb JD, Turk-Browne NB. A Taxonomy of External and Internal Attention.
820 *Annu Rev Psychol*. 2011;62(1):73-101. doi:10.1146/annurev.psych.093008.100427

821 74. Flores LE, Eckstrand KL, Silk JS, et al. Adolescents' neural response to social reward and real-
822 world emotional closeness and positive affect. *Cogn Affect Behav Neurosci*. 2018;18(4):705-717.
823 doi:10.3758/s13415-018-0598-0

824 75. Forbes EE, Hariri AR, Martin SL, et al. Altered Striatal Activation Predicting Real-World
825 Positive Affect in Adolescent Major Depressive Disorder. *Am J Psychiatry*. 2009;166(1):64-73.
826 doi:10.1176/appi.ajp.2008.07081336

827 76. Van Duijvenvoorde ACK, Peters S, Braams BR, Crone EA. What motivates adolescents?
828 Neural responses to rewards and their influence on adolescents' risk taking, learning, and cognitive
829 control. *Neurosci Biobehav Rev*. 2016;70:135-147. doi:10.1016/j.neubiorev.2016.06.037

830 77. Guyer AE, Pérez-Edgar K, Crone EA. Opportunities for Neurodevelopmental Plasticity From
831 Infancy Through Early Adulthood. *Child Dev*. 2018;89(3):687-697. doi:10.1111/cdev.13073

832 78. Lindquist KA, MacCormack JK, Shablack H. The role of language in emotion: predictions
833 from psychological constructionism. *Front Psychol*. 2015;6. doi:10.3389/fpsyg.2015.00444

834 79. Hamilton JP, Furman DJ, Chang C, Thomason ME, Dennis E, Gotlib IH. Default-Mode and
835 Task-Positive Network Activity in Major Depressive Disorder: Implications for Adaptive and
836 Maladaptive Rumination. *Biol Psychiatry*. 2011;70(4):327-333.
837 doi:10.1016/j.biopsych.2011.02.003

838 80. Nolen-Hoeksema S, Wisco BE, Lyubomirsky S. Rethinking Rumination. *Perspect Psychol Sci*.
839 2008;3(5):400-424. doi:10.1111/j.1745-6924.2008.00088.x

840 81. McEwen BS. Physiology and Neurobiology of Stress and Adaptation: Central Role of the Brain.
841 *Physiol Rev*. 2007;87(3):873-904. doi:10.1152/physrev.00041.2006

842 82. Poldrack RA. Is "efficiency" a useful concept in cognitive neuroscience? *Dev Cogn Neurosci*.
843 2015;11:12-17. doi:10.1016/j.dcn.2014.06.001

844 83. Bonanno GA, Burton CL. Regulatory Flexibility: An Individual Differences Perspective on
845 Coping and Emotion Regulation. *Perspect Psychol Sci*. 2013;8(6):591-612.
846 doi:10.1177/1745691613504116

847 84. Aldao A, Sheppes G, Gross JJ. Emotion Regulation Flexibility. *Cogn Ther Res*.
848 2015;39(3):263-278. doi:10.1007/s10608-014-9662-4

849 85. Callicott JH. Physiological Characteristics of Capacity Constraints in Working Memory as
850 Revealed by Functional MRI. *Cereb Cortex*. 1999;9(1):20-26. doi:10.1093/cercor/9.1.20

851 86. Reuter-Lorenz PA, Cappell KA. Neurocognitive Aging and the Compensation Hypothesis.
852 *Curr Dir Psychol Sci*. 2008;17(3):177-182. doi:10.1111/j.1467-8721.2008.00570.x

853 87. Viviani R, Grön G, Spitzer M. Functional principal component analysis of fMRI data. *Hum*
854 *Brain Mapp*. 2005;24(2):109-129. doi:10.1002/hbm.20074

855 88. Smith SM, Hyvärinen A, Varoquaux G, Miller KL, Beckmann CF. Group-PCA for very large
856 fMRI datasets. *NeuroImage*. 2014;101:738-749. doi:10.1016/j.neuroimage.2014.07.051

857 89. Zhang L, Xue G. Diverse and large-scale brain data in child development research. *Nat Hum*

858 *Behav*. 2025;9(6):1070-1072. doi:10.1038/s41562-025-02186-6

859 90. Esteban O, Markiewicz CJ, Blair RW, et al. fMRIPrep: a robust preprocessing pipeline for
860 functional MRI. *Nat Methods*. 2019;16(1):111-116. doi:10.1038/s41592-018-0235-4

861 91. Friston KJ. *Statistical Parametric Mapping: The Analysis of Functional Brain Images*. 1st ed.
862 Elsevier / Academic Press; 2007.

863 92. Gao X, Maurer D. A happy story: Developmental changes in children's sensitivity to facial
864 expressions of varying intensities. *J Exp Child Psychol*. 2010;107(2):67-86.
865 doi:10.1016/j.jecp.2010.05.003

866 93. Camacho MC, Williams EM, Ding K, Perlman SB. Multimodal examination of emotion
867 processing systems associated with negative affectivity across early childhood. *Dev Cogn Neurosci*.
868 2021;48:100917. doi:10.1016/j.dcn.2021.100917

869 94. Gross JJ, John OP. Individual differences in two emotion regulation processes: Implications
870 for affect, relationships, and well-being. *J Pers Soc Psychol*. 2003;85(2):348-362.
871 doi:10.1037/0022-3514.85.2.348

872 95. Spitzer RL, Kroenke K, Williams JBW, Löwe B. A Brief Measure for Assessing Generalized
873 Anxiety Disorder: The GAD-7. *Arch Intern Med*. 2006;166(10):1092.
874 doi:10.1001/archinte.166.10.1092

875 96. Kroenke K, Spitzer RL, Williams JBW. The PHQ-9: Validity of a brief depression severity
876 measure. *J Gen Intern Med*. 2001;16(9):606-613. doi:10.1046/j.1525-1497.2001.016009606.x

877 97. Watson D, Clark LA, Tellegen A. Development and validation of brief measures of positive
878 and negative affect: The PANAS scales. *J Pers Soc Psychol*. 1988;54(6):1063-1070.
879 doi:10.1037/0022-3514.54.6.1063

880 98. Achenbach TM, Ruffle TM. The Child Behavior Checklist and Related Forms for Assessing
881 Behavioral/Emotional Problems and Competencies. *Pediatr Rev*. 2000;21(8):265-271.
882 doi:10.1542/pir.21.8.265

883 99. Dodge KA, Coie JD. Social-information-processing factors in reactive and proactive

884 aggression in children's peer groups. *J Pers Soc Psychol*. 1987;53(6):1146-1158. doi:10.1037/0022-
885 3514.53.6.1146

886 100. Poldrack RA, Mumford JA, Schonberg T, Kalar D, Barman B, Yarkoni T. Discovering
887 Relations Between Mind, Brain, and Mental Disorders Using Topic Mapping. Sporns O, ed. *PLoS*
888 *Comput Biol*. 2012;8(10):e1002707. doi:10.1371/journal.pcbi.1002707

889

Supplementary Files

This is a list of supplementary files associated with this preprint. Click to download.

- Supplementarymaterials.docx